
Layer Collapse in Diffusion Language Models

Alexander Conzelmann^{1,2} Albert Catalan-Tatjer^{1,2,3} Shiwei Liu^{1,2,3}

¹Tübingen AI Center

²Max Planck Institute for Intelligent Systems

³ELLIS Institute Tübingen

Correspondence to: a.conzelmann@uni-tuebingen.de

Abstract

Diffusion language models (DLMs) have recently emerged as competitive alternatives to autoregressive (AR) language models, yet the differences in their activation dynamics remain poorly understood. We characterize these dynamics in LLaDA-8B and identify a striking layer-collapse property: a few early layers exhibit highly similar, collapsed activation patterns dominated by a single large super-outlier that persists over a long token range. Despite its apparent redundancy, we have found that this outlier is critical: pruning it causes the model’s outputs to degrade into repetitive random token loops. Paradoxically, besides this outlier, layers in LLaDA contain more redundant representations, where redundancy is particularly pronounced in earlier layers. This pattern is the reverse of what is commonly observed in AR language models, where deeper layers tend to become more redundant due to undertraining, as measured by representation similarity. Our analysis further indicates that layer collapse in DLMs is not driven by undertraining. Rather, it appears to arise from overtraining: a dominant outlier becomes an indispensable carrier of information, while the remaining representations collapse into redundant structure. These observations have strong practical implications, as we verify through controlled pre-training experiments. First, DLMs are surprisingly robust to compression: performance of LLaDA under 3-bit GPTQ quantization drops only by -1.8% on GSM8K, whereas Llama-3.1-8B under the same settings drops by -64.7%. Second, optimal non-uniform sparsity allocation reverses between the two model families: under an average budget of 50% sparsity, allocating more sparsity to early layers in LLaDA yields +8.4% over the reverse strategy, while for Llama the same early-layer-sparse allocation incurs -8.4%. Our findings reveal that the DLM training objective fundamentally reshapes layer dynamics relative to AR models, with direct consequences for how such models should be compressed and deployed. Our code is available at <https://github.com/Conzel/super-outlier-dlm>.

1 Introduction

Diffusion language models (DLMs) have recently emerged as a competitive alternative to autoregressive (AR) large language models. Open models such as LLaDA-8B [Nie et al., 2026] and DREAM-7B [Ye et al., 2025] match the quality of AR counterparts at comparable scale on standard reasoning and language understanding benchmarks. Rather than producing one token at a time from left to right, DLMs denoise a masked sequence over multiple refinement steps, which enables parallel token generation [Wu et al., 2026, Chen et al., 2026, Ma et al., 2025] and avoids the reversal curse [Berglund et al., 2024]. As DLMs become more widespread, questions on the structure of their internal representations and how they propagate through layers arise. Of particular interest is whether the findings from AR models transfer one-to-one to DLMs or if there are particular behaviours that necessitate extra care during tasks such as training, fine-tuning or compression.

In this paper, we find that DLMs show distinct and partly opposite behaviour from AR models. We find that LLaDA-8B’s internal representations are qualitatively unlike those of any AR model

previously studied. Most strikingly, a *single* activation channel (see Figure 1) remains persistently and highly activated across all tokens throughout the first half of the model’s layers — an extreme outlier that drives layer collapse, causing multiple layers to produce nearly identical, redundant hidden representations. This channel dominates the model to such a degree that ablating it alone causes a near-total collapse in capability. While outlier channels are prominent in AR models (see Dettmers et al. [2022], Yu et al. [2025]), they only cause extreme activations for specific tokens or token positions, and pruning a single one of them causes only a noticeable accuracy drop (-4% in our experiment, see Table 1), but not complete model collapse. The layer-wise similarity structure is also inverted (see Figure 3). In standard AR models, early layers usually learn more distinct transformations, while deeper layers become increasingly redundant as a consequence of undertraining [Sun et al., 2026]. By contrast, LLaDA-8B exhibits highly redundant early layers. We find that this redundancy is driven by the dominating super-outlier, which suppresses the representation expressivity of other channels across the first few layers.

At first glance, this observation conflicts with the curse-of-depth hypothesis [Sun et al., 2026], which attributes high representation similarity in Pre-LN Transformers to the undertraining of deeper layers. However, our weight spectral density analysis shows that DLMs exhibit a compatible layerwise trainability pattern, but with a different source of redundancy. In LLaDA-8B, the unusually high similarity among early layers is not caused by undertraining; instead, it arises from the relative overtraining of these layers, resulting in dominant super-outliers concentrated in the earliest layers.

Why activation structure matters. A long line of work has shown that algorithms which explicitly account for activation structure [Lin et al., 2024, Lee et al., 2024, Ashkboos et al., 2024] substantially outperform naive counterparts on quantization and pruning. The structure itself has been mapped in detail for AR models: *outlier features*, extreme activations found in essentially all sufficiently large language models [Dettmers et al., 2022, An et al., 2025], are tied to core information-processing functions. *Super-weights* suppress stop-tokens [Yu et al., 2025], and attention outliers at sequence boundaries serve as sinks for excess attention mass [Gu et al., 2025, Xiao et al., 2024]. Early DLM work hints that the picture is different: Rulli et al. [2025] report that attention sinks are present in DLMs but far less sensitive to removal, an observation that Myrzakhan et al. [2026] have already exploited for more efficient pruning. Our results push this line considerably further, and identify the diffusion training objective itself as the source of the divergence.

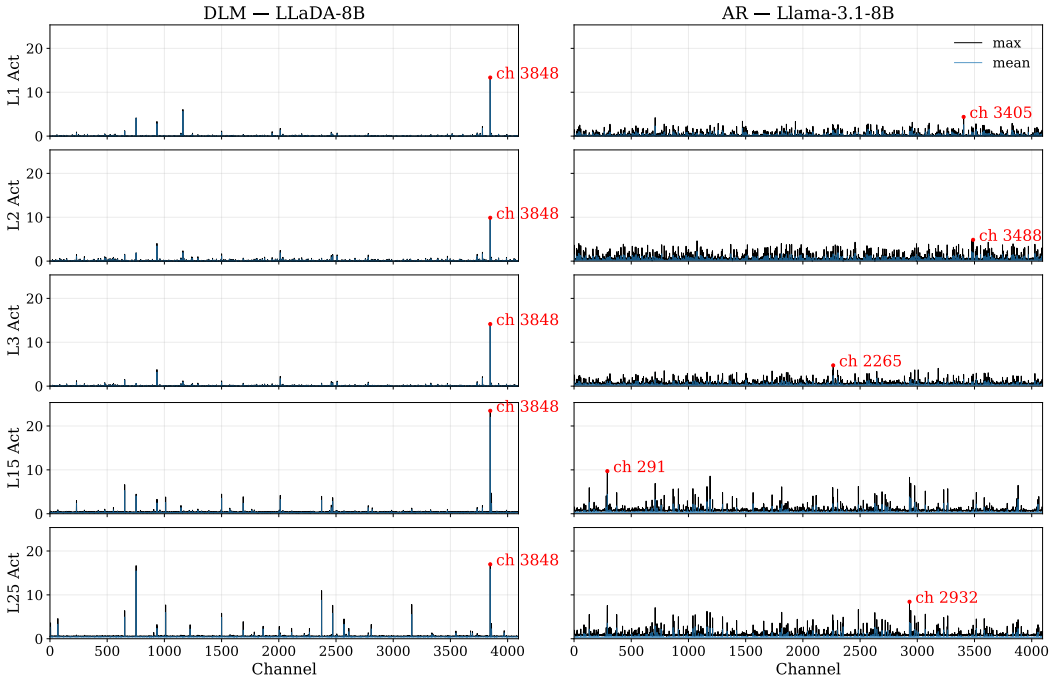


Figure 1: LLaDA activations contain a single consistent, very large super-outlier channel which persists well into the middle layers. The marked dot shows the channel with the highest activation magnitude maximum (averaged over tokens and sequence positions). For Llama, the dominant channel changes on almost every layer.

Contributions. We close part of the knowledge gap between AR and diffusion language models through a systematic study of activation histograms and layer similarities in LLaDA-8B. To separate effects arising from the diffusion objective from architectural quirks, we compare LLaDA-8B to Llama-3.1-8B, which share a near-identical architecture, and complement this with the first controlled pre-training comparison in which an AR and a DL model are trained under identical conditions.

- We identify a *super-outlier* in LLaDA-8B: a single dominant activation channel qualitatively distinct from the weight and activation outliers previously reported in AR LLMs, and whose removal collapses the model.
- We characterize the layer-similarity structure of LLaDA-8B and show that it differs markedly from that of comparable AR models, with early layers being highly redundant rather than distinct, corroborated by weight spectral analysis indicative of significant overfitting.
- We translate these observations into practical guidance for DLM compression and show that AR-derived sparsity heuristics are not merely suboptimal but actively inverted relative to what LLaDA-8B calls for.
- To isolate the role of the training objective, we pre-train an AR and a DL model under an identical setup and show that the diffusion objective is responsible for the observed layer and compression behaviours. To our knowledge, this is the first such controlled comparison.

2 Layer Dynamics in Diffusion Language Models

2.1 Metrics

Layer Similarity. Our main method of analysis is the per-token cosine similarity between the hidden activations of different layers of a model. Let $h_i(x, t) \in \mathbb{R}^d$ denote the hidden state at layer i for input sequence $x \sim p_x$ at token position t . We define the layer-wise similarity as

$$\text{sim}(i, j) = \mathbb{E}_{x \sim p_x} \mathbb{E}_t \left[\frac{\langle h_i(x, t), h_j(x, t) \rangle}{\|h_i(x, t)\|_2 \|h_j(x, t)\|_2} \right], \quad (1)$$

where the inner expectation is taken over all (non-padding) token positions t in the sequence. A value of $\text{sim}(i, j)$ close to 1 indicates that layers i and j produce nearly collinear representations, which we use as a proxy for layer redundancy: if the representation barely changes between two layers, the intermediate computation contributes little and is a natural candidate for pruning.

Estimating Activations. In practice, we estimate all hidden layer activations using a fixed calibration set of 128 sequences of length 2048 drawn from the C4 corpus. For DLMs we duplicate each sample 4 times and mask a $t \sim \text{Unif}[0, 1]$ fraction of tokens to imitate the activation statistics of a partly decoded sample sequence. We note however that this has very little effect on the resulting figures (see subsection B.1, repeating similarity and activation plots without masking), indicating that our findings are not sensitive to the exact decoding process that the DLM implements.

Heavy-tailedness of the Weight Spectrum as a Layer Trainability Measure. Representation similarity is a useful diagnostic for identifying redundant layers, but it is not by itself a reliable measure of layer trainability. High similarity can arise from qualitatively different mechanisms: in AR Transformers, similar representations in deeper layers are often associated with under-trained, near-identity residual mappings [Sun et al., 2026], whereas in DLMs, highly similar layers may instead reflect strong training of a few dominant directions, manifested as distinguished spectral or activation outliers. Thus, similarity-based importance metrics can be misleading, since they conflate under-utilized layers with layers whose representations are highly structured but dominated by a small number of directions.

Motivated by Heavy-Tailed Self-Regularization (HT-SR) theory [Martin and Mahoney, 2019, Lu et al., 2024, He et al., 2026], we argue that the heavy-tailedness of the weight spectrum provides a more reliable, training-data-free measure of layer quality than representation similarity. HT-SR theory suggests that the empirical spectral density of neural-network weight matrices encodes information about the degree of learned structure: heavier-tailed spectra are typically associated with stronger feature learning and better-trained layers. In our setting, this spectral perspective is particularly useful because it helps distinguish two cases that representation similarity alone cannot separate: near-identity redundancy caused by insufficient training, and apparent redundancy caused by strong low-dimensional structure or outlier-dominated spectra.

To quantify the heavy-tailedness of a layer, we use the Hill estimator α_{Hill} [Lu et al., 2024]. For weight W , let $\lambda_1 \geq \lambda_2 \geq \dots \geq \lambda_N$ denote the eigenvalues of $W^\top W$ sorted in decreasing order.

The Hill estimator of the power-law tail exponent, computed from the top k eigenvalues, is

$$\alpha_{\text{Hill}}(k) = 1 + \frac{k}{\sum_{i=1}^k \log \frac{\lambda_{n-i+1}}{\lambda_{n-k}}}, \quad (2)$$

where smaller values of α_{Hill} indicate heavier-tailed spectra. We set k using the fix-finger method [Yang et al., 2023]. Under HT-SR theory, a heavier tail is typically interpreted as evidence of stronger feature learning.

2.2 Super-Outlier in LLaDA-8B

Activation outliers are a well observed phenomenon in LLMs, but those spikes usually only occur briefly for specific tokens or for specific token positions [An et al., 2025]. In the case of LLaDA-8B, we present a unique finding: when analyzing the activation heatmaps over sequence positions in LLaDA, we find that there exists one single dominant outlier channel, which has a persistently high activation (up to 5 times as large as the next largest outlier) over all sequence positions (see Figure 2).

In contrast to outliers in AR models, which are reported to have well behaved mechanisms such as stop-word suppression [Yu et al., 2025], the super-outlier in LLaDA seems more akin to a constant bias that is learned by the network. The qualitative effect of pruning the super-outlier is striking: LLaDA-8B degenerates into repetitive token loops, regardless of the prompt. As an illustrative example (taken from GSM8K):

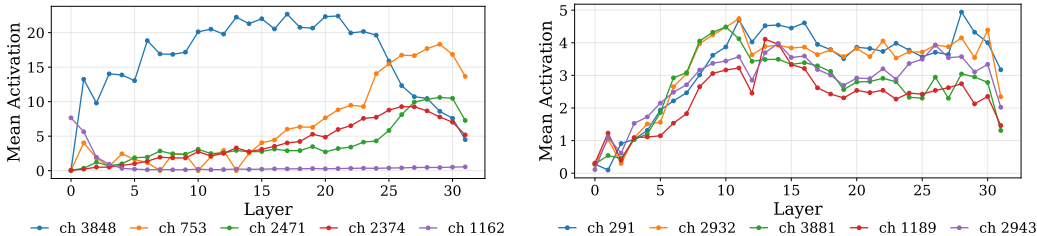
Question. Kylar went to the store to buy glasses for his new apartment. One glass costs \$5, but every second glass costs only 60% of the price. Kylar wants to buy 16 glasses. How much does he need to pay for them?

LLaDA-8B answer (super-outlier pruned). *buy buy buy buy!yl buy buy buy*

This is in stark contrast to Llama-3.1-8B, where removing the highest magnitude channel only slightly reduces the accuracy, see Table 1.

Table 1: Effect of pruning the single highest-magnitude channel on GSM8K (small subset). Removing channel 3848 in LLaDA-8B (the super-outlier) collapses the model entirely, while pruning the corresponding top-magnitude channel in Llama-3.1-8B causes only a minor accuracy drop.

Model	Channel pruned	Accuracy	Δ baseline
Llama-3.1-8B	291	79%	-4%
LLaDA-8B	3848	0%	-83%



(a) LLaDA-8B: the super-outlier channel dominates the top-5 magnitudes consistently across early-middle layers. (b) Llama-3.1-8B: top-5 channels are of comparable magnitude; dominant channel changes across layers.

Figure 2: Magnitudes of the top-5 QKV input channels across layers. In LLaDA-8B, one channel persistently dominates by a wide margin, whereas in Llama-3.1-8B no single channel is dominant.

2.3 Early-Layer Redundancies in LLaDA-8B

Next, we analyze the pairwise similarities of the hidden representations in LLaDA and Llama in Figure 3. Surprisingly, we find that almost all layers in LLaDA (top left) exhibit an extremely high similarity to each other, especially early layers which are almost identical to each other even over ranges of 15+ layers. This is partially mitigated if the similarities are calculated with the channel corresponding to the super-outlier set to zero (Ch. 3848, see subsection 2.2), but the learned representations for LLaDA are still more redundant than the ones from Llama-3.1-8B (which will result in a stronger robustness of DLMS compared to ARs, see section 3). On the other hand, for

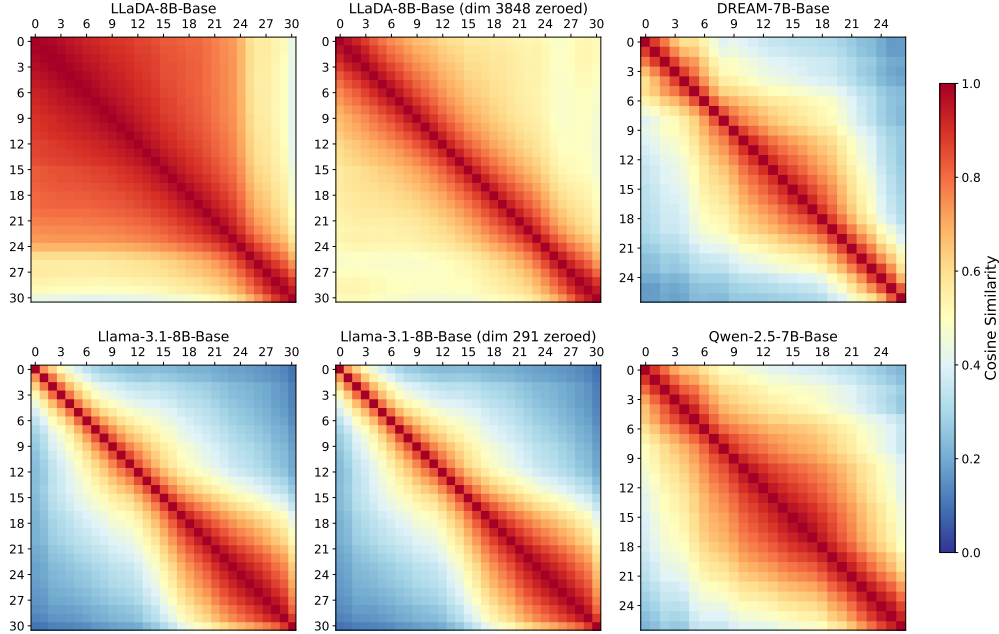


Figure 3: Per-token cosine similarity for different models. The top row shows DLMs, the bottom shows ARs. The left column shows a comparison of LLaDA-8B and Llama-3.1-8B, where LLaDA-8B exhibits highly redundant (collapsed) layer similarities. For the middle column, we have removed the largest outlier from the similarity calculations, showing that much of the layer similarity of LLaDA is due to a single outlier, unlike Llama, where removing one outlier barely changes the resulting similarities. The right column shows a comparison between Qwen-2.5-7B and DREAM-7B. As DREAM was finetuned from Qwen-initialized weights, their layer similarity patterns are very similar.

Llama-3.1-8B (bottom left), the early layers show very distinct activation patterns, and the later layers contain more redundancy, in line with previous work on AR models.

This behaviour from LLaDA-8B is not shared with DREAM-7B, since DREAM has been initialized from the weights of Qwen-2.5-7B (an AR model) and only fine-tuned on masked sequences. Therefore, the final weights of DREAM do not differ much from the ones of Qwen, and their similarity patterns look almost identical. This outlier profile can be harmful in handling DLMs. Common wisdom is that strong outliers make for layers or networks that are hard to compress; thus the compression community has devised various ways of dealing with them [Lin et al., 2024, Dettmers et al., 2022, Ashkboos et al., 2024]. Based on this, metrics such as OWL [Yin et al., 2025] allocate a lower sparsity level to layers with strong outliers (which are presumably difficult to compress). In LLaDA-8B, this would mean that early layers should be pruned less aggressively. Due to the redundancy that is exhibited in the early layers, we have a different finding: early layers can actually be pruned more strongly; we quantify this in section 3.

2.4 Heavy-Tailed Evidence of Overtraining

Leveraging the analysis performed by Martin and Mahoney [2019], Lu et al. [2024], we can also measure how well trained the layers in a neural network are via the α_{Hill} estimator.

According to the works of [Zhou et al., 2023, Liu et al., 2024, He et al., 2025], a balanced distribution of α_{Hill} indicates, that the layers in a network are better trained. A relatively low value of α_{Hill} (with respect to the other layers) indicates a relatively "overtrained" layer, while a very high value of α_{Hill} indicates an "undertrained" layer.

This behaviour can be seen in Figure 4: early layers in LLaDA-8B have a strikingly low α_{Hill} (relative) value, while the distribution of the twin-model Llama-3.1-8B is much more flat. This ties in with the early-layer occurrence of the super-outlier, a form of over-training where the layer representations collapse to a single dominant channel.

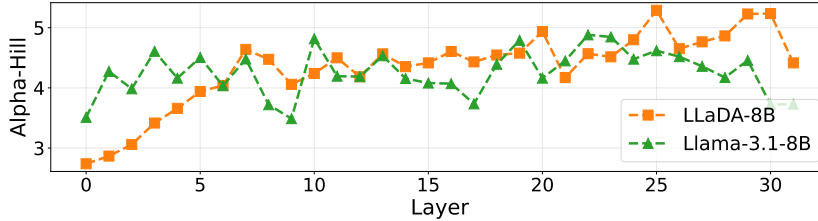


Figure 4: The α_{Hill} value is very low in the early layers of LLaDA-8B which shows that these layers are actually overtrained. α_{Hill} is averaged over modules in layer.

3 DLMs Are More Robust to Compression Despite Super-Outliers

In this section, we demonstrate that our observations have practically relevant consequences when dealing with DLMs. For this, we have chosen the task of model compression. We prune and quantize LLaDA and Llama-3.1-8B using GPTQ and WANDA and measure their performance on math and question-answering under different overall and layer-wise compression strength allocations. We show that (a) AR-optimal schemes for layer-wise compression strength are inverted when dealing with DLMs and (b) DLMs have more compression robustness. Observation (a) is a direct consequence of our layer-wise similarity analysis, but observation (b) is particularly surprising, as LLaDA-8B contains a super-outlier that is very sensitive to change. However, we have seen in Figure 1 that LLaDA contains fewer outliers apart from the super-outlier, and we have seen in Figure 3 that LLaDA layer activations are more redundant, even when the outlier is removed. This translates to an overall stronger compression robustness, particularly as modern compression methods (like WANDA) are designed to be robust to a certain amount of outliers.

3.1 Experiment Setup

Evaluation. Models are evaluated both on an average of 6 common question-answering (QnA) tasks (ARC-C, HellaSwag, PIQA, Winogrande, BoolQ, OBQA) as well as on reasoning via GSM8K. DLMs are evaluated using FastDLLM [Wu et al., 2026] with a generation length of 1024 and one token decoded per diffusion step. Further details can be found in subsection A.1.

Compression. Pruning experiments were performed using WANDA [Sun et al., 2024b] and quantization experiments using GPTQ [Frantar et al., 2023]. Both methods used calibration samples drawn from the C4 dataset (128 for WANDA, 256 for GPTQ). Adding samples with masked tokens did not change the performance of the compression at all, so we opted not to mask samples for the DLM compression. The described sparsity schedules *earlier-is-sparser* (EIS) and *deeper-is-sparser* (DIS) follow a simple linear allocation, using an ϵ of 0.08. This means for EIS applied to a T layer network at sparsity s , we assign sparsity $s + 0.08 \left(1 - \frac{2(t-1)}{T-1}\right)$ to layer t . Correspondingly, for DIS, the addition turns into a subtraction.

3.2 Compression

Pruning. Our experiments in Figure 5 (top row) show the average accuracy on QnA tasks (left) respectively GSM8K reasoning (right) of LLaDA-8B and Llama-3.1-8B at three sparsity levels (0.3, 0.5, 0.7) and under three sparsity allocation strategies that result in the same total sparsity (uniform, earlier-is-sparser, deeper-is-sparser).

These results reinforce the practicality of our observations made in section 2. We have two key observations to make in the results: **First**, LLaDA starts out with a generally lower accuracy than Llama, but is much more robust when compressed achieving almost double the accuracy of Llama for GSM8K at 50% sparsity. This ties into our observation that Llama-3.1-8B contains many more similarities, introducing redundancy into the network and making the accuracy of each single layer less important (as long as the super-outlier is protected, which is exactly the case under WANDA pruning). **Second**, the optimal sparsity allocation differs between LLaDA and Llama. For Llama, pruning early layers more strongly (EIS) is always suboptimal and either uniform sparsity allocation or pruning deeper layers more strongly (DIS) are the optimal choice (depending on task). For LLaDA, this flips, and DIS is usually the suboptimal choice, with either EIS or uniform performing the best. Only for sparsity 0.7 on QnA, DIS significantly outperforms EIS for LLaDA, which we suspect

might be due to the fact that the very high sparsity level starts to necessitate pruning of the weights connected to the super-outlier.

Quantization. As quantization is usually the more practical method of compressing a neural network, we have included experiments on quantization as well in Figure 5 (bottom row). However, as quantization has to be done to discrete bit widths, we have not included an experiment on a layerwise bit-width allocation, which cannot be made with such a fine-grained allocation as is done in the experiments on pruning.

Other than that, these experiments reinforce the same observation we have made for pruning above, namely that LLaDA is inherently more robust to compression than Llama-3.1-8B, starting out with a worse base performance and surpassing the performance of Llama at 3 bit for QnA (left figure) and already at 4 bit for GSM8K (right figure).

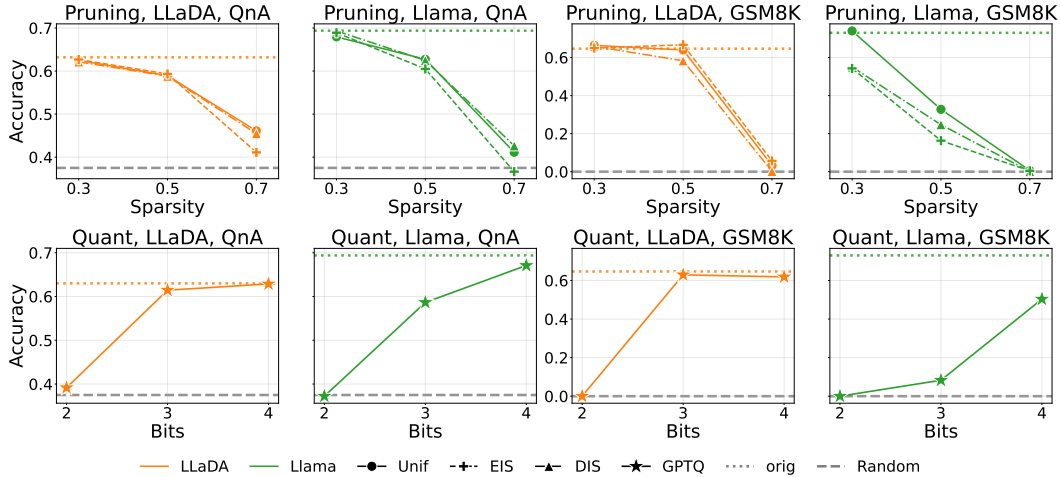


Figure 5: Compression performance for LLaDA-8B and Llama-3.1-8B: pruning across sparsity allocation strategies (top row, at $\epsilon = 0.08$) and GPTQ quantization across bit-widths (bottom row), evaluated on the base-model commonsense QnA tasks (left column) and the instruct-model GSM8K task (right column).

4 Supporting Evidence: A Controlled 160M Pair

The experiments in this section reinforce that our findings are not just a spurious quirk of LLaDA-8B, but are inherent to the pre-training objective that is used in DLMs. To establish this, we perform pre-training experiments with a Pythia-160M [Vaswani et al., 2017, Biderman et al., 2023] architecture pre-trained on 100B tokens from FineWebEdu [Penedo et al., 2024]. The resulting models AR-160M, DLM-160M are trained identically, solely varying in the training objective (cross-entropy either with or without masking). Further details are in subsection A.2. We perform the same evaluation as we did for section 3, minus GSM8K due to the small model scale.

4.1 Results

Our analysis of the small-scale models supports the following two observations from the base model: (a) early layer representations in DLM-160M are more similar to each other than in AR-160M, and more similar to each other than the deeper layer representations, and (b) DLM-160M shows more robustness to compression than AR-160M. Due to our controlled setting, we could thus ensure that these observations are due to the DLM training objective and not due to architectural or pre-training hyperparameter choices. We note that DLM-160M is lacking the super-outlier: to observe weight and activation outliers, one has to train models to much larger scale ($>6.7B$ indicated by Dettmers et al. [2022]), which was out of the scope of this work.

Layer Similarities. To more easily quantify how similar the layer representations in our two models are, we have averaged the per-layer similarities in a blockwise fashion: we have grouped the first 4 layers of the model together, as well as the last 4 layers and have averaged over the resulting 16 inner-block layer-wise similarities. Table 2 shows that the same early-layer redundancy pattern of the large models starts to emerge in our pre-trained models: the early layer similarity is higher in DLM-160M compared to AR-160M, while it flips for the late-layer similarities.

Table 2: Average cosine-similarities between early layers are higher for DLM-160M. To better assess the similarity, we have grouped the first 4 layers and the last 4 layers together and have averaged over their pairwise cosine similarities.

Model	Early-layer similarity	Deeper-layer similarity
DLM-160M	0.877	0.787
AR-160M	0.818	0.829

Heavy-tailed Signature. The same heavy-tailed signature appears in the 160M pair (Figure 6): the controlled DLM shows a markedly lower α_{Hill} in early layers, while its AR twin does not. This behaviour normalizes in later layers, where both models show similar α_{Hill} values.

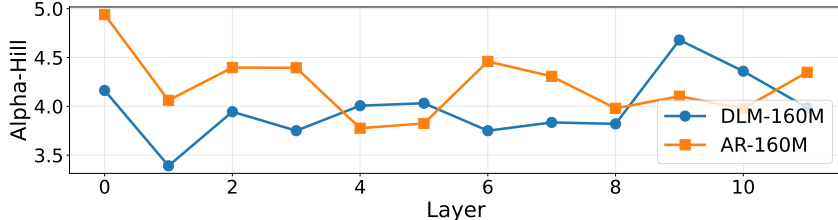


Figure 6: Similar to the larger models, α_{Hill} is smaller for DLM-160M compared to AR-160M.

Compression Results. In Figure 7, we present results for pruning (left) and quantization (right) of our 160M models. We have performed pruning and evaluation for all pre-training learning rates and selected the best performing model per sparsity level. Similar to the behaviour of LLaDA-8B, DLM-160M starts out with less performance than AR-160M, but is more robust to compression. Here, the DLM model only supersedes its AR counterpart for the quantization experiment, while for pruning, they roughly match at the highest sparsity level (which could be due to initially subpar performance of DLM-160M). Also replicating the behaviour of LLaDA versus Llama, the best sparsity allocation strategy for DLM-160M is consistently earlier-is-sparser, while AR-160M achieves higher accuracy using deeper-is-sparser (aside from low sparsity regimes up to 40%, where all strategies perform similarly). This matches the expectations from our similarity analysis in Table 2.

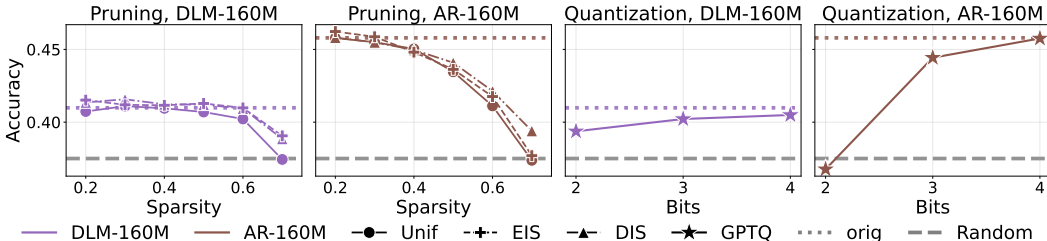


Figure 7: Robustness replication on the controlled 160M pair: pruning (left) and quantization (right). DLM-160M loses less performance than AR-160M under pruning, with the best sparsity allocation strategy inverted (EIS for the DLM, DIS for the AR). Under quantization, DLM-160M starts below AR-160M at full precision but surpasses it from 2 bits onward. Both results are in line with the behaviour of LLaDA-8B versus Llama-3.1-8B.

5 Related Work

Outliers, Sinks, and Super-weights. A growing body of work shows that a small number of coordinates disproportionately shape large language model behaviour. Attention sinks concentrate probability mass on a handful of tokens [Xiao et al., 2024, Gu et al., 2025]; massive activations identify a few token positions whose hidden states grow orders of magnitude larger than the rest [Sun et al., 2024a]; super weights [Yu et al., 2025] and systematic outliers [An et al., 2025] extend the picture to individual parameters and feature dimensions whose removal disproportionately damages the model. These phenomena are predominantly described along the *token* axis: a small set of positions dominates attention or activation norm. Collapsed layers describe the *channel-axis* counterpart: a single hidden dimension that dominates the representation across all positions. In contrast to attention sinks, this phenomenon is absent in autoregressive models of comparable scale.

Curse of Depth. Multiple works analyze the tendency of AR models to have less well-trained deeper layers [Sun et al., 2026, Gromov et al., 2025, Siji et al., 2026], a phenomenon also termed the *Curse of Depth*. Existing approaches to mitigate this issue include depth-growing during training [Kapl et al., 2025], adding sparsity to the model [Muhtar et al., 2026] or mixing Pre- and Post-LN [Li et al., 2024]. While our work reveals that early layers in DLMs are more redundant and can be compressed more strongly than in ARs, this does not mean that the curse is broken: if an improved training paradigm would make early-layers more informative and distinct, DLMs still exhibit strong redundancies in later layers and could thus face similar issues.

Weight and Activation Dynamics in DLMs. A concurrent work by Goel et al. [2026] also uses the cosine-similarity of hidden-states to characterize layer-dynamics, but analyzes similarities between immediately neighbored layers instead of long-range interactions, also revealing early-layer redundancies. The authors use this to propose a layer-skip method for inference, which is different from our sparsity allocation. In agreement with our work, the authors find that AR-finetuned DLMs retain most of the layer dynamics from initialization. Apart from that, our work uses cosine similarities in a markedly different way, which allows us to detect the super-outlier in LLaDA-8B. Additionally, we provide controlled AR-DLM twins and perform extensive compression experiments. Rulli et al. [2025] characterise attention sinks in DLMs, which are token-level attention outliers. Our work is complementary, as we analyze channel-wide *activation* outliers.

Compression of Diffusion Language Models. Several recent works compress masked diffusion language models. On the quantization side, DLM-Quant [Xu and Yang, 2025], Quant-dLLM [Zhang et al., 2026], and Lin et al. [2025] adapt post-training quantization pipelines to the bidirectional, multi-step inference of DLMs. Myrzakhan et al. [2026] use insights on attention sinks in DLMs to improve pruning. These works treat compression as a methodological problem, where they adapt a known technique to a new architecture. Our work is decidedly not a compression paper, but an analysis of activation dynamics whose findings carry practical implications that may be used in further compression research.

6 Discussion

We have shown that DLMs exhibit activation dynamics that are qualitatively distinct from their AR counterparts. LLaDA-8B contains a single dominant activation channel that persists across all token positions and early layers; removing it causes total model collapse, a fragility with no parallel in AR models of comparable scale. This super-outlier drives early-layer redundancy through a mechanism we attribute to overtraining rather than undertraining, as evidenced by heavy-tailed weight spectra in early layers. A controlled 160M pre-training comparison supports that both the redundancy pattern and the compression robustness are products of the diffusion training objective and not architectural or pre-training artifacts. These findings carry direct practical consequences: Allocating more sparsity to deeper layers, exactly what is useful for AR models, instead performs suboptimally on DLMs.

We envision that our findings inspire further research into DLM activation dynamics. The super-outlier in particular leaves many open questions, for example, which mechanisms of the DLM pre-training process produce it, and whether it is a harmful artifact or provides a useful role in information processing of DLMs. Additionally, the redundancy of DLM layer representations might indicate that the pre-training process is not yet optimized, similar to how redundant later layers in pre-LN AR models indicate suboptimal gradient flow. Ensuring that all layers are trained to produce distinct and informative representations would produce models that are more capable at similar sizes.

Limitations. Our findings are mostly focussed on a single DLM-AR pair, namely LLaDA-8B and Llama-3.1-8B. While the behaviour of Llama-3.1-8B is consistent with what is reported in the AR model literature, our findings for LLaDA-8B are novel. To our knowledge, LLaDA-8B is the only large-scale DLM that is completely pre-trained from scratch, as the current literature is mostly focussed on creating DLMs by fine-tuning them from AR model weights [Bie et al., 2025, 2026, Yu et al., 2026]. During fine-tuning, these models’ weights stay close to their original, therefore models such as DREAM-7B show activation dynamics that are very close to their AR counterpart, see Figure 3. While supporting our other findings, the 160M pre-training models did not show the super-outlier as LLaDA-8B, which was expected given the small scale of the model. To make our results more widely applicable, a large-scale DLM pre-training study could be implemented, pre-training DLMs on multiple parameter scales (e.g. 350M, 1B, 3B, 8B, 16B). This task unfortunately requires large amounts of GPU resources to run.

References

- N. Ajroldi. plainLM: Language model pretraining in PyTorch. <https://github.com/Niccolo-Ajroldi/plainLM>, 2024.
- Y. An, X. Zhao, T. Yu, M. Tang, and J. Wang. Systematic outliers in large language models. In *The Thirteenth International Conference on Learning Representations*, 2025.
- S. Ashkboos, A. Mohtashami, M. L. Croci, B. Li, P. Cameron, M. Jaggi, D. Alistarh, T. Hoeffler, and J. Hensman. QuaRot: Outlier-free 4-bit inference in rotated llms. In A. Globerson, L. Mackey, D. Belgrave, A. Fan, U. Paquet, J. Tomczak, and C. Zhang, editors, *Advances in Neural Information Processing Systems*, volume 37, pages 100213–100240. Curran Associates, Inc., 2024. doi: 10.52202/079017-3180.
- L. Berglund, M. Tong, M. Kaufmann, M. Balesni, A. C. Stickland, T. Korbak, and O. Evans. The Reversal Curse: LLMs trained on “A is B” fail to learn “B is A”. In *The Twelfth International Conference on Learning Representations*, 2024.
- S. Bergsma, N. Dey, G. Gosal, G. Gray, D. Soboleva, and J. Hestness. Straight to zero: Why linearly decaying the learning rate to zero works best for llms, 2025. URL <https://arxiv.org/abs/2502.15938>.
- S. Biderman, H. Schoelkopf, Q. G. Anthony, H. Bradley, K. O’Brien, E. Hallahan, M. A. Khan, S. Purohit, U. S. Prashanth, E. Raff, A. Skowron, L. Sutawika, and O. Van Der Wal. Pythia: A suite for analyzing large language models across training and scaling. In *Proceedings of the 40th International Conference on Machine Learning (ICML)*, volume 202, pages 2397–2430. PMLR, 2023. doi: 10.48550/arXiv.2304.01373.
- T. Bie, M. Cao, K. Chen, L. Du, M. Gong, Z. Gong, Y. Gu, J. Hu, Z. Huang, Z. Lan, C. Li, C. Li, J. Li, Z. Li, H. Liu, L. Liu, G. Lu, X. Lu, Y. Ma, J. Tan, L. Wei, J.-R. Wen, Y. Xing, X. Zhang, J. Zhao, D. Zheng, J. Zhou, J. Zhou, Z. Zhou, L. Zhu, and Y. Zhuang. LLaDA2.0: Scaling up diffusion language models to 100B, 2025.
- T. Bie, M. Cao, X. Cao, B. Chen, F. Chen, K. Chen, L. Du, D. Feng, H. Feng, M. Gong, Z. Gong, Y. Gu, J. Guan, K. Guan, H. He, Z. Huang, J. Jiang, Z. Jiang, Z. Lan, C. Li, J. Li, Z. Li, H. Liu, L. Liu, G. Lu, Y. Lu, Y. Ma, X. Mou, Z. Pan, K. Qiu, Y. Ren, J. Tan, Y. Tian, Z. Wang, L. Wei, T. Wu, Y. Xing, W. Ye, L. Zha, T. Zhang, X. Zhang, J. Zhao, D. Zheng, H. Zhong, W. Zhong, J. Zhou, J. Zhou, L. Zhu, M. Zhu, and Y. Zhuang. LLaDA2.1: Speeding up text diffusion via token editing, 2026.
- Y. Bisk, R. Zellers, R. L. Bras, J. Gao, and Y. Choi. PIQA: Reasoning about physical commonsense in natural language, 2019.
- Z. Chen, G. Fang, X. Ma, R. Yu, and X. Wang. dParallel: Learnable parallel decoding for dLLMs. In *The Fourteenth International Conference on Learning Representations*, 2026.
- C. Clark, K. Lee, M.-W. Chang, T. Kwiatkowski, M. Collins, and K. Toutanova. BoolQ: Exploring the surprising difficulty of natural yes/no questions. In J. Burstein, C. Doran, and T. Solorio, editors, *Proceedings of the 2019 Conference of the North American Chapter of the Association for Computational Linguistics: Human Language Technologies, Volume 1 (Long and Short Papers)*, pages 2924–2936, Minneapolis, Minnesota, June 2019. Association for Computational Linguistics. doi: 10.18653/v1/N19-1300.
- P. Clark, I. Cowhey, O. Etzioni, T. Khot, A. Sabharwal, C. Schoenick, and O. Tafjord. Think you have solved question answering? Try ARC, the AI2 reasoning challenge, 2018.
- K. Cobbe, V. Kosaraju, M. Bavarian, M. Chen, H. Jun, L. Kaiser, M. Plappert, J. Tworek, J. Hilton, R. Nakano, C. Hesse, and J. Schulman. Training verifiers to solve math word problems. *arXiv preprint arXiv:2110.14168*, 2021.
- T. Dettmers, M. Lewis, Y. Belkada, and L. Zettlemoyer. Gpt3.int8(): 8-bit matrix multiplication for transformers at scale. In S. Koyejo, S. Mohamed, A. Agarwal, D. Belgrave, K. Cho, and A. Oh, editors, *Advances in Neural Information Processing Systems*, volume 35, pages 30318–30332. Curran Associates, Inc., 2022.

- E. Frantar, S. Ashkboos, T. Hoefler, and D. Alistarh. Gptq: Accurate post-training quantization for generative pre-trained transformers, 2023. URL <https://arxiv.org/abs/2210.17323>.
- L. Gao, J. Tow, B. Abbasi, S. Biderman, S. Black, A. DiPofi, C. Foster, L. Golding, J. Hsu, A. Le Noac’h, H. Li, K. McDonell, N. Muennighoff, C. Ociepa, J. Phang, L. Reynolds, H. Schoelkopf, A. Skowron, L. Sutawika, E. Tang, A. Thite, B. Wang, K. Wang, and A. Zou. The language model evaluation harness, July 2024.
- R. Goel, R. Garrepalli, S. Agrawal, C. Lott, M. Lee, and F. Porikli. A comparative analysis of layer-wise representational capacity in AR and diffusion llms, 2026.
- A. Gromov, K. Tirumala, H. Shapourian, P. Glorioso, and D. Roberts. The unreasonable ineffectiveness of the deeper layers. In *The Thirteenth International Conference on Learning Representations*, 2025.
- X. Gu, T. Pang, C. Du, Q. Liu, F. Zhang, C. Du, Y. Wang, and M. Lin. When attention sink emerges in language models: An empirical view. In *The Thirteenth International Conference on Learning Representations*, 2025.
- D. He, S. Tu, A. Jaiswal, L. Shen, G. Yuan, S. Liu, and L. Yin. AlphaDecay: Module-wise weight decay for heavy-tailed balancing in llms, 2025.
- D. He, S. Tu, K. Wang, L. Yin, and S. Liu. One LR doesn’t fit all: Heavy-tail guided layerwise learning rates for LLMs. In *Proceedings of the International Conference on Machine Learning (ICML)*, 2026. URL <https://openreview.net/forum?id=Aj3ZWgxYwt>.
- F. Kapl, E. Angelis, T. Hoppe, K. Maile, J. von Oswald, N. Scherrer, and S. Bauer. Do depth-grown models overcome the curse of depth? An in-depth analysis. *ArXiv*, abs/2512.08819, 2025.
- D. P. Kingma and J. Ba. Adam: A method for stochastic optimization. In *International Conference on Learning Representations (ICLR)*, 2015. URL <https://arxiv.org/abs/1412.6980>.
- W. Kwon, Z. Li, S. Zhuang, Y. Sheng, L. Zheng, C. H. Yu, J. E. Gonzalez, H. Zhang, and I. Stoica. Efficient memory management for large language model serving with PagedAttention. In *Proceedings of the ACM SIGOPS 29th Symposium on Operating Systems Principles*, 2023.
- C. Lee, J. Jin, T. Kim, H. Kim, and E. Park. OWQ: Outlier-aware weight quantization for efficient fine-tuning and inference of large language models, 2024.
- P. Li, L. Yin, and S. Liu. Mix-LN: Unleashing the power of deeper layers by combining pre-LN and post-LN. *ArXiv*, abs/2412.13795, 2024.
- H. Lin, H. Xu, Y. Wu, Z. Guo, R. Zhang, Z. Lu, Y. Wei, Q. Zhang, and Z. Sun. Quantization Meets dLLMs: A Systematic Study of Post-training Quantization for Diffusion LLMs, Oct. 2025.
- J. Lin, J. Tang, H. Tang, S. Yang, W.-M. Chen, W.-C. Wang, G. Xiao, X. Dang, C. Gan, and S. Han. AWQ: Activation-aware weight quantization for LLM compression and acceleration. In *MLSys*, 2024.
- Z. Liu, Y. Hu, T. Pang, Y. Zhou, P. Ren, and Y. Yang. Model balancing helps low-data training and fine-tuning. In Y. Al-Onaizan, M. Bansal, and Y.-N. Chen, editors, *Proceedings of the 2024 Conference on Empirical Methods in Natural Language Processing*, pages 1311–1331, Miami, Florida, USA, Nov. 2024. Association for Computational Linguistics. doi: 10.18653/v1/2024.emnlp-main.78.
- I. Loshchilov and F. Hutter. Decoupled weight decay regularization. In *International Conference on Learning Representations (ICLR)*, 2019. URL <https://arxiv.org/abs/1711.05101>.
- A. Lou, C. Feng, S. Ermon, and J. Zhao. Discrete diffusion modeling by estimating the ratios of the transition kernel. In *Proceedings of the 41st International Conference on Machine Learning (ICML)*, 2024. URL <https://arxiv.org/abs/2310.16834>.
- H. Lu, Y. Zhou, S. Liu, Z. Wang, M. W. Mahoney, and Y. Yang. AlphaPruning: Using heavy-tailed self regularization theory for improved layer-wise pruning of large language models. In *The Thirty-Eighth Annual Conference on Neural Information Processing Systems*, 2024.

- Y. Ma, L. Du, L. Wei, K. Chen, Q. Xu, K. Wang, G. Feng, G. Lu, L. Liu, X. Qi, X. Zhang, Z. Tao, H. Feng, Z. Jiang, Y. Xu, Z. Huang, Y. Zhuang, H. Xu, J. Hu, Z. Lan, J. Zhao, J. Li, and D. Zheng. dInfer: An Efficient Inference Framework for Diffusion Language Models, Oct. 2025.
- C. H. Martin and M. W. Mahoney. Traditional and Heavy-Tailed Self Regularization in Neural Network Models, Jan. 2019.
- T. Mihaylov, P. Clark, T. Khot, and A. Sabharwal. Can a suit of armor conduct electricity? A new dataset for open book question answering. In *EMNLP*, 2018.
- D. Muhtar, X. Song, S. Pokutta, M. Zimmer, N. Pelleriti, T. Hofmann, and S. Liu. When does sparsity mitigate the curse of depth in llms, 2026.
- A. Myrzakhan, T. Li, B. Guo, S. Tang, and Z. Shen. Sink-aware pruning for diffusion language models, 2026.
- S. Nie, F. Zhu, Z. You, X. Zhang, J. Ou, J. Hu, JUN. ZHOU, Y. Lin, J.-R. Wen, and C. Li. Large language diffusion models. In *The Thirty-Ninth Annual Conference on Neural Information Processing Systems*, 2026.
- G. Penedo, H. Kydlíček, L. Cappelli, M. Žilínek, C. Chapman, C. Guest, L. Guntupalli, A. Bakouch, I. Malartic, H. Touvron, et al. The FineWeb datasets: Decanting the web for the finest text data at scale. *arXiv preprint arXiv:2406.17557*, 2024. URL <https://arxiv.org/abs/2406.17557>.
- M. E. Rulli, S. Petrucci, E. Michielon, F. Silvestri, S. Scardapane, and A. Devoto. Attention sinks in diffusion language models, 2025.
- S. Sahoo, A. Lou, R. Chen, and V. Kuleshov. Simple and effective masked diffusion language models. In *Advances in Neural Information Processing Systems (NeurIPS)*, 2024. URL <https://arxiv.org/abs/2406.07524>.
- K. Sakaguchi, R. L. Bras, C. Bhagavatula, and Y. Choi. WinoGrande: An adversarial winograd schema challenge at scale, 2019.
- A. Siji, A. M. Karimi-Mamaghan, F. Kapl, T. Höppe, E. Angelis, A. Dittadi, M. Brenner, M. Heinzinger, K. H. Johansson, K. Maile, J. von Oswald, and S. Bauer. From words to amino acids: Does the curse of depth persist? *ArXiv*, abs/2602.21750, 2026.
- M. Sun, X. Chen, J. Z. Kolter, and Z. Liu. Massive activations in large language models. In *First Conference on Language Modeling*, 2024a.
- M. Sun, Z. Liu, A. Bair, and J. Z. Kolter. A simple and effective pruning approach for large language models. In *The Twelfth International Conference on Learning Representations*, 2024b.
- W. Sun, X. Song, P. Li, L. Yin, Y. Zheng, and S. Liu. The curse of depth in large language models. In *The Thirty-Ninth Annual Conference on Neural Information Processing Systems*, 2026.
- A. Vaswani, N. Shazeer, N. Parmar, J. Uszkoreit, L. Jones, A. N. Gomez, Ł. Kaiser, and I. Polosukhin. Attention is all you need. In *Advances in Neural Information Processing Systems (NeurIPS)*, pages 5998–6008, 2017. URL <https://papers.nips.cc/paper/7181-attention-is-all-you-need>.
- K. Wen, Z. Li, J. Wang, D. Hall, P. Liang, and T. Ma. Understanding warmup-stable-decay learning rates: A river valley loss landscape perspective. *arXiv preprint arXiv:2410.05192*, 2024.
- C. Wu, H. Zhang, S. Xue, Z. Liu, S. Diao, L. Zhu, P. Luo, S. Han, and E. Xie. Fast-dLLM: Training-free acceleration of diffusion LLM by enabling KV cache and parallel decoding. In *The Fourteenth International Conference on Learning Representations*, 2026.
- G. Xiao, Y. Tian, B. Chen, S. Han, and M. Lewis. Efficient streaming language models with attention sinks. In *The Twelfth International Conference on Learning Representations*, 2024.
- C. Xu and D. Yang. DLLMQuant: Quantizing Diffusion-based Large Language Models, Aug. 2025.

- Y. Yang, R. Theisen, L. Hodgkinson, J. E. Gonzalez, K. Ramchandran, C. H. Martin, and M. W. Mahoney. Test accuracy vs. generalization gap: Model selection in NLP without accessing training or testing data. In *Proceedings of the 29th ACM SIGKDD Conference on Knowledge Discovery and Data Mining*, Kdd '23, pages 3011–3021, New York, NY, USA, 2023. Association for Computing Machinery. ISBN 979-8-4007-0103-0. doi: 10.1145/3580305.3599518.
- J. Ye, Z. Xie, L. Zheng, J. Gao, Z. Wu, X. Jiang, Z. Li, and L. Kong. Dream 7B: Diffusion Large Language Models, Aug. 2025.
- L. Yin, Y. Wu, Z. Zhang, C.-Y. Hsieh, Y. Wang, Y. Jia, G. Li, A. Jaiswal, M. Pechenizkiy, Y. Liang, M. Bendersky, Z. Wang, and S. Liu. Outlier Weighed Layerwise Sparsity (OWL): A Missing Secret Sauce for Pruning LLMs to High Sparsity, June 2025.
- M. Yu, D. Wang, Q. Shan, C. J. Reed, and A. Wan. The super weight in large language models, 2025.
- Y. Yu, Y. Jian, J. Wang, Z. Zhou, D. Zhuang, X. Fang, S. Yanamandra, X. Wu, Q. Wu, S. L. Song, T. Dao, B. Athiwaratkun, J. Zou, F. Lai, and C. Xu. Introspective diffusion language models, 2026.
- R. Zellers, A. Holtzman, Y. Bisk, A. Farhadi, and Y. Choi. HellaSwag: Can a machine really finish your sentence?, 2019.
- T. Zhang, Z. Li, X. Yan, H. Qin, Y. Guo, and Y. Zhang. Quant-dLLM: Post-training extreme low-bit quantization for diffusion large language models. In *The Fourteenth International Conference on Learning Representations*, 2026.
- Y. Zhou, T. Pang, K. Liu, c. h martin, M. W. Mahoney, and Y. Yang. Temperature balancing, layer-wise weight analysis, and neural network training. In *Thirty-Seventh Conference on Neural Information Processing Systems*, 2023.

A Experimental details

A.1 Evaluation of Language Models

Models are evaluated on the following question-answering tasks: ARC-Challenge Clark et al. [2018], HellaSwag Zellers et al. [2019], PIQA Bisk et al. [2019] WinoGrande Sakaguchi et al. [2019], BoolQ Clark et al. [2019], OpenbookQA Mihaylov et al. [2018]. Additionally, we evaluate on reasoning via GSM8K [Cobbe et al., 2021]. We use 25-shot for ARC-Challenge, 10-shot for HellaSwag, 5-shot for WinoGrande and GSM8K, and 0-shot for BoolQ, OpenBookQA, and PIQA. We used base models for QnA, and corresponding instruction-finetuned variants for GSM8K.

For the DLMs, we used an adapted version FastDLM [Wu et al., 2026] with single KV-cache, but not parallel decoding. The block-length was set to 32 and the generation length to 1024, with 1024 decoding steps (so 1 token per decoding step) and low confidence remasking. For the AR models, we use vLLM [Kwon et al., 2023] for inference acceleration together with LM-Eval [Gao et al., 2024].

All evaluations are done on a single H100 GPU. Evaluations take around 6 hours for DLMs and 20 minutes for AR models for both task sets.

A.2 Small-scale pre-training

Autoregressive Model. We used Ajroldi [2024] to pretrain Pythia-160M parameter transformer models [Vaswani et al., 2017, Biderman et al., 2023] on causal language modeling, with 100B tokens of FineWebEdu [Penedo et al., 2024] on $8 \times A100$ -80GB GPUs. We use sequence length 2048 and a batch size of 0.5M tokens, cross-entropy loss, Adam [Kingma and Ba, 2015] with decoupled weight decay [Loshchilov and Hutter, 2019] of 0.1, gradient clipping of 1, and $(\beta_1, \beta_2) = (0.9, 0.95)$. We use Warm up-Stable-Decay [Wen et al., 2024] to schedule the learning rates, warm up of 1900 steps (1%) and decay to 0 [Bergsma et al., 2025] of 10% of token budget. We perform three independent runs for learning rates $\{3 \times 10^{-3}, 1 \times 10^{-3}, 3 \times 10^{-4}\}$.

Diffusion Language Model. We adapt this pipeline into a Masked Discrete Diffusion Language Model [MDLM; Sahoo et al., 2024, Lou et al., 2024] trainer with four modifications: (i) a bidirectional attention patch on the GPTNeoX backbone, (ii) a forward absorbing-state corruption step, (iii) an

importance-weighted cross-entropy loss applied only at corrupted positions, and (iv) the reuse of an unused vocabulary slot as the [MASK] token. All other hyperparameters, including data order, are identical to the AR trainer.

B Further experiment plots

B.1 Activations and similarities without masking

We replicate a subset of our experiments while calculating activations in DLMs without masking tokens to showcase that our findings are robust over diffusion steps.

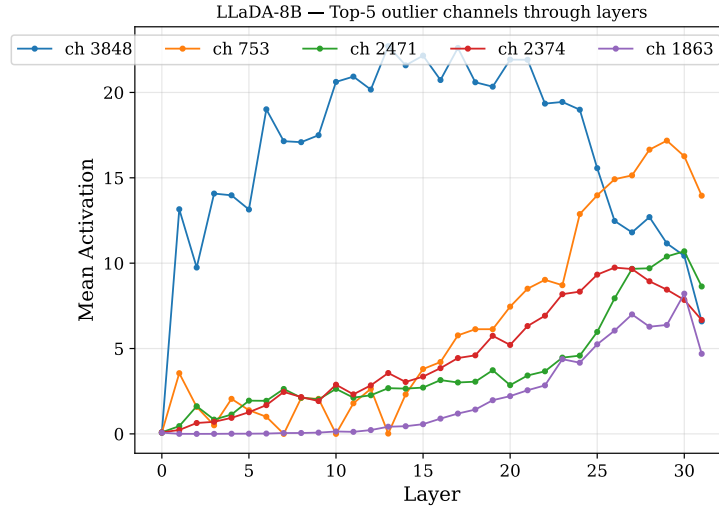


Figure 8: Similar to Figure 2a, but without including masked sequences.

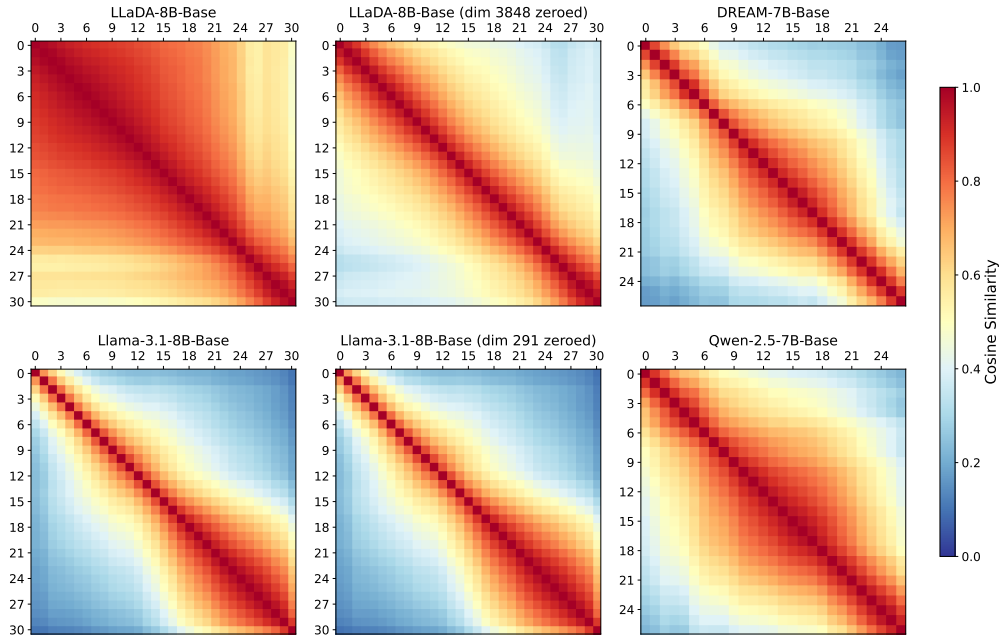


Figure 9: Similar to Figure 3, but without including masked sequences.

B.2 Extended activation plots

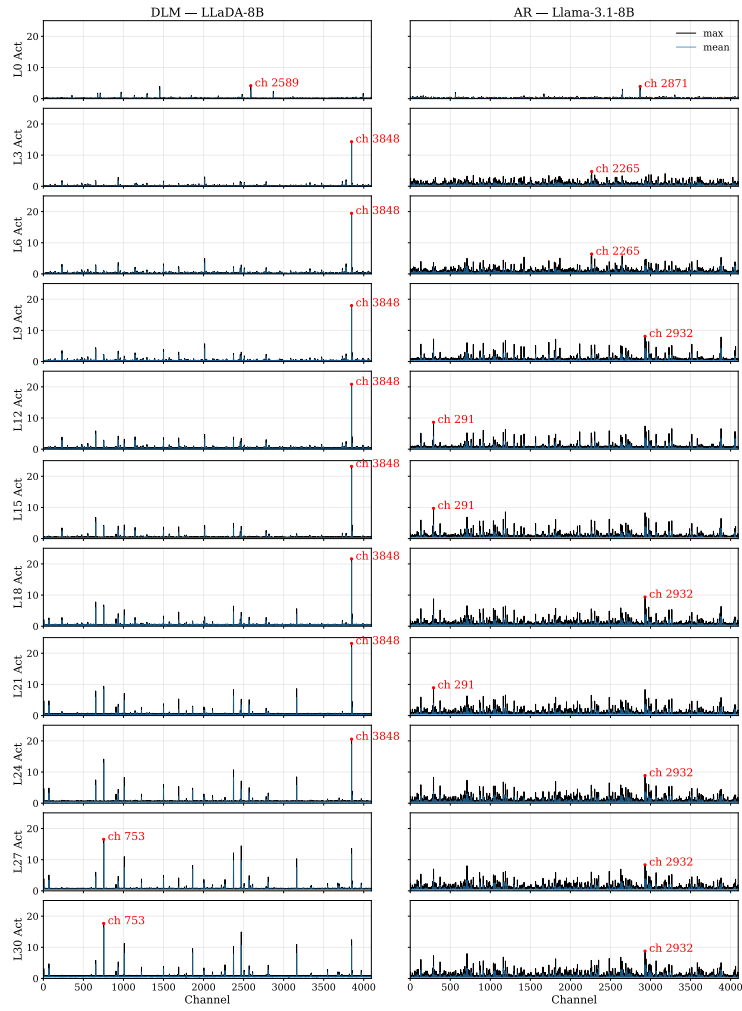


Figure 10: Extended version of Figure 1.

B.3 Channel activation over Diffusion Steps

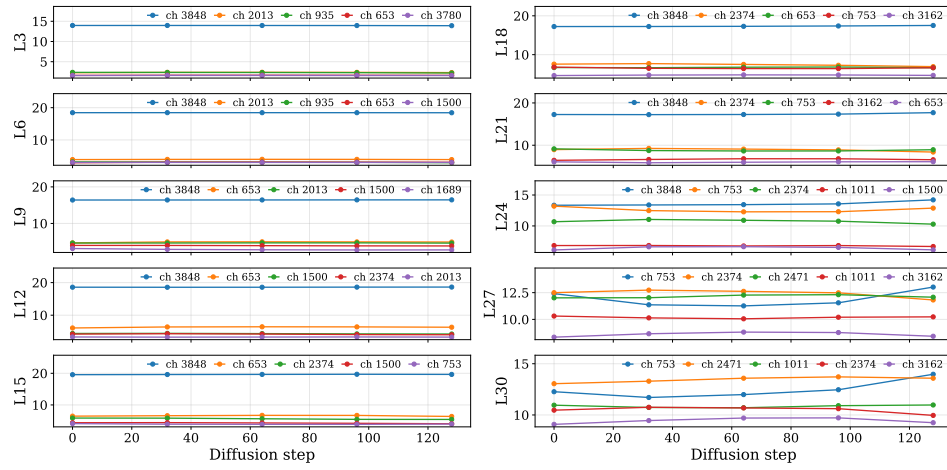


Figure 11: Channel magnitude mean of the top-5 largest (by mean) channels in LLaDA-8B, over different diffusion steps. The channel magnitudes for early-mid layers barely change over the diffusion step.